

# The Influence of Stabilizer Concentration on the Mechanical Properties of Alumina – 17 vol% Zirconia (0.6Y-2Y) Composites

F. Kern\*, S. Koummarasy, R. Gadow

University of Stuttgart, IFKB, Allmandring 7B, D-70569 Stuttgart Germany

received May 2, 2016; received in revised form May 10, 2016; accepted June 15, 2016

## Abstract

Zirconia-toughened alumina (ZTA) with a zirconia content close to the percolation threshold has become the state-of-the-art ceramic material for hip implants. In this study the stabilizer content in a ZTA with 17 vol% zirconia was varied between 0.6–2 mol%  $Y_2O_3$  to understand more about the influence of the stabilizer concentration on mechanical properties, phase composition and formation of residual stress. It was found that fracture resistance reaches its maximum close to the stress neutral state where transformation stresses equilibrate residual cooling stresses while compressive stress in the alumina matrix favors higher strength.

*Keywords:* Ceramics, mechanical properties, zirconia, alumina, residual stress

## I. Introduction

The mechanical properties of alumina, which is frequently used as a structural ceramic due to its high hardness, abrasion resistance and moderate price, can be significantly enhanced with the addition of second phases. Among these composite ceramics, ZTA (zirconia-toughened alumina) is probably the most widespread material with applications ranging from mechanical engineering in e.g. tribologically loaded machine elements or cutting tools for machining of grey-cast iron<sup>1,2</sup>. Since 2003, a platelet-reinforced zirconia-toughened alumina composite (Bio-Lox Delta®) has become the benchmark material in joint replacement owing to its mechanical properties and high ageing resistance<sup>3,4,5</sup>. The reinforcing mechanisms in ZTA are transformation toughening, microcracking and crack deflection by residual stress fields<sup>6</sup>. The first ZTA materials exploited the redistribution of the crack energy by permanent microcracks which were introduced by means of the addition of large unstabilized zirconia particles which retransform to monoclinic during cooling<sup>7</sup>. While this leads to high toughness, the strength suffers considerably from a weakening of the microstructure. ZTA materials with high strength can be obtained with zirconia dispersions that retain the tetragonal phase during cooling from sintering temperature<sup>8</sup>. This can be achieved by either limiting the fraction of zirconia to approximately 10 %, thus forming a non-percolating dispersion or by stabilizing the zirconia added in larger fractions with the addition of yttria<sup>8</sup>. These tetragonal particles in the wake of a proceeding crack can be transformed to monoclinic, which is associated with volume expansion and shear leading to a reduction of the stress intensity at the crack tip<sup>9</sup>. In combination with transformation toughening, microcracking can occur, which further helps dissipation

of the crack energy. The transformability of the tetragonal inclusions basically depends on their size, stabilizer content and location in the microstructure<sup>10</sup>. Compared to Y-TZP, the transformability of the zirconia is reduced by the constraint of the alumina matrix, which has a higher stiffness than zirconia. As in real ZTA materials, the zirconia grain sizes have a certain size range. Some large grains may retransform to monoclinic while the majority stays tetragonal, the smallest grains remain untransformable even under applied stress. The role of homogeneity resulting from choice of starting powders and processing has been highlighted by Gregori<sup>11</sup>, they measured the residual stresses in ZTA by means of piezo spectroscopy depending on the variations in feedstock processing and elaborated a calculation scheme for the hydrostatic residual stress in the alumina matrix depending on the amount of zirconia transformed. Systematic studies on the properties of ZTA materials with variation of zirconia content and stabilizer are relatively rare, most of the materials investigated up until now were either ZTA materials without stabilizer<sup>12</sup> or ZTA materials with 3Y-TZP as a dispersion which is untransformable and derives its toughness from residual stress effects alone<sup>13</sup>. A study was recently published by Exare covering ZTA materials with a wide range of stabilizer contents in the dispersion (from monoclinic to cubic zirconia), however, with most compositions far off the optimum for high-performance ZTA<sup>14</sup>. In two publications by Sommer, a 3 x 3 x 3 parameter matrix with 10, 17 and 24 % zirconia, 1 mol%, 1.5 mol% and 2 mol% yttria and sintering times of 1–3 h at 1475 °C was covered. It was shown that superior properties can only be reached for very specific combinations of these parameters<sup>15,16</sup>. The grid was, however, too coarse to see effects in the vicinity of the optimum of mechanical properties which was located at 17 vol% zirconia with 1 mol% yttria stabi-

\* Corresponding author: [frank.kern@ifkb.uni-stuttgart.de](mailto:frank.kern@ifkb.uni-stuttgart.de)

lizer. This study aims at clarifying the effects of stabilizer content variation in the vicinity of the optimum detected by Sommer with a sufficiently high resolution. Therefore, a composition typical for biomedical grade ZTA with zirconia content at the percolation point was chosen and the stabilizer content was varied between 0.6 mol% and 2 mol% in 0.2 mol% increments.

## II. Materials and Methods

The starting powders for the present study are the same as reported by Sommer. Submicron-size  $\alpha$ -alumina APA 0.5 (Ceralox, USA) with a particle size of 300 nm and a specific surface area of 8 m<sup>2</sup>/g. For the zirconia monoclinic nanopowder TZ-0 (Tosoh, Japan) with a specific surface area of 17 m<sup>2</sup>/g and a mean crystallite size of  $\sim$ 30 nm<sup>15</sup> was coated with 3 mol% yttria via the nitrate route. The exact procedure for that is reported elsewhere<sup>17</sup>. The different stabilizer concentrations of 0.6–2 mol% were produced from this stabilizer-coated 3Y-TZP and plain TZ-0 by blending. Batches of 150 g of the commensurate amounts of the three powders were attrition-milled in 2-propanol using 3Y-TZP milling balls of 2 mm in diameter for 2 h. E.g. the 17ZTA1Y was made by blending 114.2 g alumina, 23.9 g unstabilized TZ-0 and 11.9 g stabilizer-coated 3Y-TZP. The resulting slurry was then dried at 85 °C overnight and screened through a 100- $\mu$ m mesh to obtain the ready-to-press powder. Sample denomination is given by the stabilizer content (e.g. 17ZTA0.6Y = ZTA with 17 vol% zirconia stabilized with 0.6 mol% yttria). Samples were consolidated at 1475 °C and 40 MPa axial pressure by hot-pressing in vacuum in boron-nitride-clad graphite dies measuring 45 mm in diameter (FCT Anlagenbau, Germany). Two samples of 2 mm in thickness were produced from each composition. After cooling down with the heater switched off, the samples were manually ground to remove the surrounding grit and then lapped with 15- $\mu$ m diamond suspension and subsequently polished with 15- $\mu$ m, 6- $\mu$ m and 1- $\mu$ m suspension for 30 min (Struers Rotopol, Denmark). The resulting disks were then cut into bars of 4 mm width using a diamond wheel (Struers Accutom 50, Denmark). The sides were then lapped with 15- $\mu$ m diamond dispersion to remove cutting grooves, the edges were beveled manually with a 40- $\mu$ m diamond disk. The characterization of the samples included the measurement of the sintered density with the buoyancy method, determination of the Young's modulus with the resonance method (IMCE, Belgium), Vickers hardness HV10 was measured by applying a load of 98.1 N for 10 s (Bareiss, Germany). Bending strength was measured by means of four-point measurement with a 20 mm outer and 10 mm inner span on a minimum of ten samples each measuring 3.5 x 2 x 25 mm<sup>3</sup> at a crosshead speed of 0.5 mm/min. Fracture resistance was determined based on direct crack length measurement (DCM) on five HV10 indents each, applying the Evans' calculation model as well as by indentation strength in a bending (ISB) test<sup>18,19</sup>. For the ISB test, four test bars each were indented with a HV10 indent in the middle of the tensile side with the cracks parallel and perpendicular to the sides. The residual strength was then measured immediately at a crosshead speed of 2.5 mm/min in the same 4pt setup (Zwick, Germany).

The phase composition of the samples was determined by means of XRD. Polished samples (an entire polished disk of 45 mm diameter) and fracture faces of samples broken in the ISB test (4–5 fragments aligned in the sample holder) were inspected with a diffractometer in a Bragg-Brentano setup using Cu K $\alpha$  radiation with a graphite monochromator (Bruker D8, Germany). For the quantification of the phase composition of the zirconia intensities of the characteristic monoclinic (-111) and (111) and tetragonal (101), reflections in the 2 theta range of 27–33 °C range were determined and the phase composition calculated using the calibration curve of Toraya<sup>20</sup>. The depth of the transformation zones and the transformation toughness increment was calculated from XRD data according to Kosmac and McMeeking<sup>21,22</sup>. The residual stress distribution was calculated analytically according to Gregori<sup>11</sup>. The microstructure of polished, thermally etched and Pd-coated surfaces of all samples was studied with in-lens SEM (Zeiss Gemini, Germany) using a low acceleration voltage of 3 kV.

## III. Results

### (1) Microstructure

All samples studied are basically fully dense and show an identical microstructural architecture. Zirconia grains of 400–500 nm size are distributed homogeneously within the alumina matrix, which has a grain size of approximately 1  $\mu$ m (Fig. 1). Zirconia grains are located predominantly at the grain boundaries; some smaller globular inclusions of zirconia can also be found inside larger alumina grains.

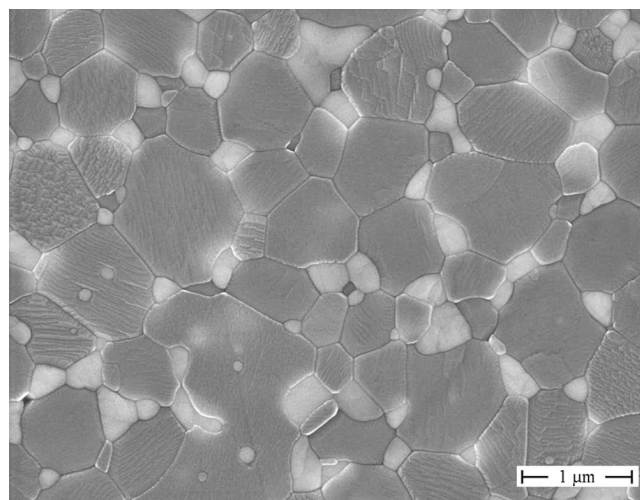


Fig. 1: Microstructure of 17ZTA1.0Y, SEM image.

One decisive difference is the predominant presence of monoclinic grains in the materials with a low stabilizer content (0.6–0.8 mol%). Monoclinic domains in zirconia can be identified by the self-accommodating twin-like orientation of transformed domains. The transformation strain leads to visible gaps, indicating a weakening of grain boundaries (Fig. 2). Surfaces in 17ZTA0.6Y are difficult to polish because grains or even grain assemblies tend to break out of the microstructure. At higher stabilizer contents > 1.2 mol%, monoclinic domains can no

longer be detected in the microstructure with SEM. At high stabilizer contents, the monoclinic grains no longer appear as individuals but as agglomerate clusters of ultra-fine (100–200 nm) grains (not shown).

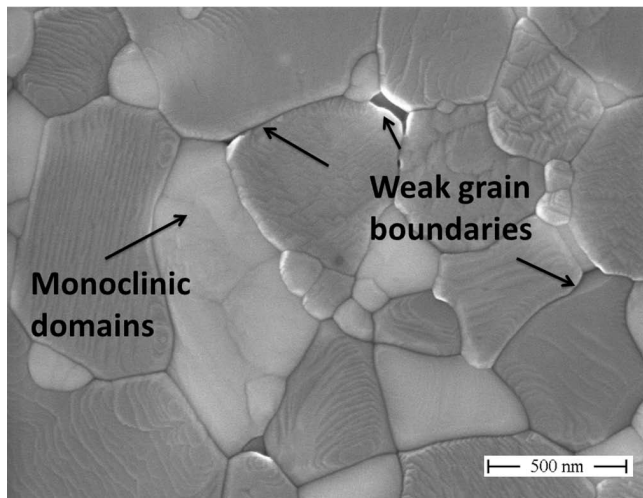


Fig. 2: Detail of the microstructure of 17ZTA0.6Y featuring monoclinic domains and weak grain boundaries as a result of transformation strain, SEM image.

(2) Phase composition and residual stress

Fig. 3 shows the monoclinic content in the polished surfaces ( $V_{m, polished}$ ), the monoclinic content in the fracture faces ( $V_{m, fractured}$ ) and the resulting transformability  $V_f$  of 17ZTA materials depending on stabilizer content. In good accord with SEM images, phase composition in polished surfaces measured by means of XRD first show a slow increase in the monoclinic fraction of zirconia with decreasing stabilizer content from 0 vol% in 17ZTA2.0Y to 8 vol% in 17ZTA1.2Y. Then monoclinic content rises exponentially, passing 20 % in 17ZTA1.0Y and 48 % in 17ZTA0.8Y to 56 % at the lowest stabilizer concentration. The transformability  $V_f$  defined as the difference between monoclinic content in fracture face and polished surface is negligible at stabilizer contents  $\geq 1.6$  mol%. Between 0.8 and 1.4 mol% a flat plateau region is formed where  $V_f = 8-10$  vol%, the transformability in 17ZTA0.6Y is zero.

It should be pointed out that zirconia phase compositions in machined surfaces may differ strongly under the influence of machining-induced process zones. Care was therefore taken to avoid any grinding processes and to reproducibly machine the surfaces by lapping and polishing under standardized, prolonged and gentle conditions with an automatic machine.

Fig. 4 shows the transformation zone size  $h$  determined according to Kosmac, the calculated transformation toughness increment according to McMeeking assuming a transformation efficiency of 0.27 (predominantly dilatonic) and the calculated hydrostatic residual stress according to Gregori<sup>21,22,23,11</sup>. Assuming a maximum transformability of 70 % in the materials the, transformation depth in the ZTA materials calculated according to Kosmac is  $\sim 2 \mu\text{m}$  for 1.0–1.4 Y,  $< 0.3 \mu\text{m}$  for higher stabilizer contents and reaches a maximum value of  $\sim 2.7 \mu\text{m}$  in 17ZTA0.8Y. The level of 70 % was not chosen on the basis of phase composition, we can assume that all com-

positions should be located in the limits of the tetragonal field at sintering temperature, but on the basis of the coincidence of maximum transformability level in polished and fractured samples in case of 17ZTA0.6Y. As Heuer has shown the ultrafine fraction of tetragonal grains as well as the intracrystalline zirconia remain untransformable even under stress and should, from the authors' understanding, be excluded from the balance<sup>10</sup>.

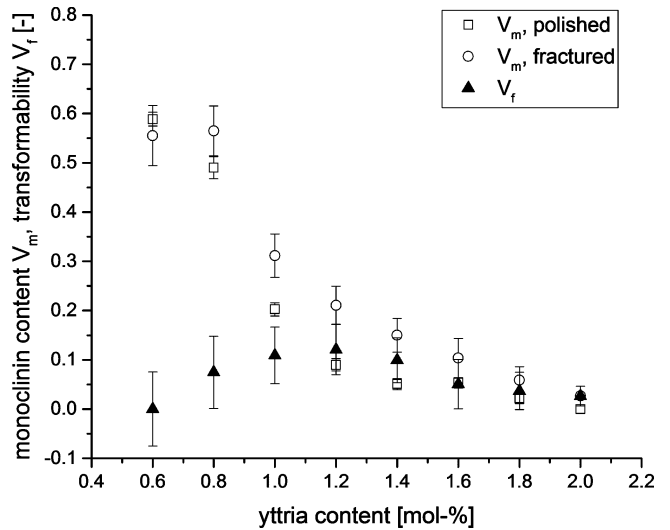


Fig. 3: Monoclinic contents in the polished surfaces  $V_{m, polished}$ , the fracture faces  $V_{m, fractured}$  and the resulting transformability  $V_f$  in 17ZTA materials depending on stabilizer content.

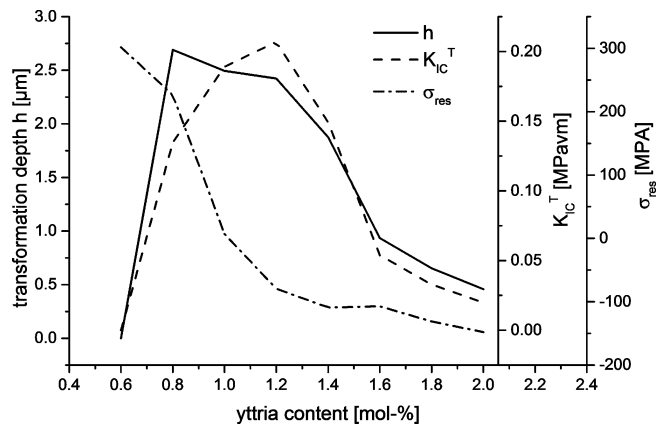


Fig. 4: Transformation zone size  $h$ , calculated transformation toughness increment  $K_{IC}^T$  and the calculated hydrostatic residual stress in the alumina matrix depending on stabilizer content in 17ZTA.

The corresponding transformation toughness increment  $\Delta K_{IC}^T$  calculated according to McMeeking is negligible above 1.6 mol%. Transformation toughness forms a plateau at  $\sim 0.15 \text{ MPa}\sqrt{\text{m}}$  at 1–1.4Y and a maximum of  $0.2 \text{ MPa}\sqrt{\text{m}}$  in 17ZTA0.8Y.

Evidently transformation toughness is not the governing factor for the increase in fracture resistance. The calculation of residual stress according to Gregori shows that 17ZTA1.0Y is perfectly stress neutral, in all compositions with higher stabilizer contents the alumina matrix is under compressive stress and vice versa.

### (3) Mechanical properties

Density and Young's modulus of ZTA materials are shown in Fig. 5. As we may expect a density of  $\sim 4.33 \text{ g/cm}^3$  from the rule of mixture, all materials can be considered fully dense. The drop in density at 0.6–0.8 mol% yttria is probably related to the higher monoclinic content in these samples. Young's modulus reaches the value expected according to the rule of mixture ( $\sim 355 \text{ GPa}$ ) and shows no statistically significant fluctuation with stabilizer content.

Hardness HV 10 and 4-pt bending strength  $\sigma_{4pt}$  of the ZTA composites is shown in Fig. 5. For both, a flat maximum in the intermediate stabilizer content range is observed. From 17ZTA0.6Y to 17ZTA1Y the hardness increases considerably from 1760 to 1860, standard deviations of hardness are relatively high in this range (40–55). In the intermediate and high stabilizer concentration range the hardness stays relatively constant at a level of 1820–1900 with standard deviations varying between 20–35. The strength of the materials shows a peak value of 940 MPa in 17ZTA1.4Y, strength is relatively stable at a level of  $> 900 \text{ MPa}$  between 1–1.6 mol% yttria and declines at higher and lower stabilizer contents. While strength declines linearly with higher stabilizer contents, it drops rather abruptly with reduction of the stabilizer content below 1 mol%. The lowest strength is observed for 17ZTA0.6Y with 600 MPa. This is probably related to the microcracks induced by the excessively high monoclinic content which represent structural flaws (see Fig. 2).

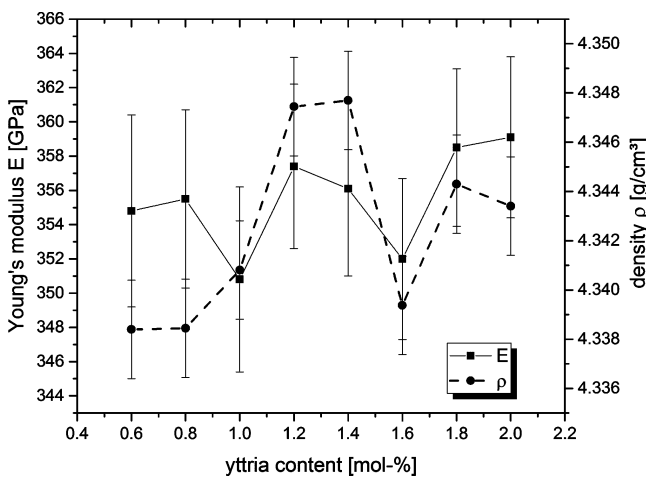


Fig. 5: Density and Young's modulus of 17ZTA materials depending on stabilizer content.

Fig. 6 shows the fracture resistance values obtained with direct crack length measurement  $K_{DCM}$  and the fracture resistance determined with the residual strength method  $K_{ISB}$ . Both basically show a similar trend. The fracture resistance of the materials measured with the residual strength method ISB shows a moderate increase from  $4 \text{ MPa}\sqrt{\text{m}}$  to  $4.6 \text{ MPa}\sqrt{\text{m}}$  with reduction of the stabilizer content from 2 mol% to 1.2 mol%. Then toughness rises significantly to a peak value of  $7.1 \text{ MPa}\sqrt{\text{m}}$  at 0.8 mol%. Further reduction of stabilizer leads to a drastic decline to  $5.2 \text{ MPa}\sqrt{\text{m}}$  in 17ZTA0.6Y. The maximum toughness determined with the DCM method is found in 17ZTA1Y,  $K_{DCM} = 7.5 \text{ MPa}\sqrt{\text{m}}$ . As Quinn has shown that DCM val-

ues should – if used at all – be interpreted cautiously, this slight shift should not be overstressed<sup>24</sup>.

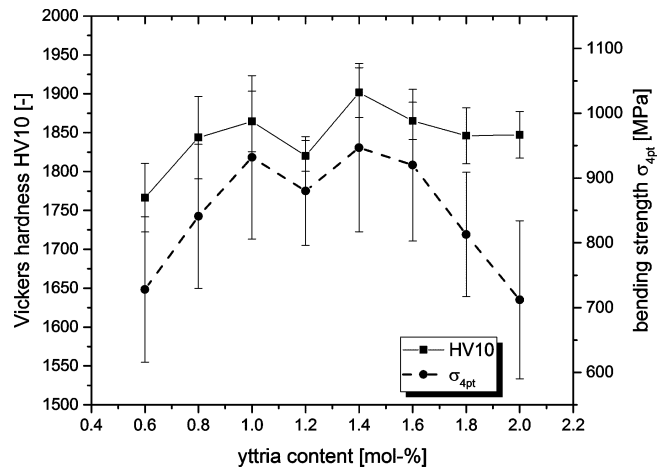


Fig. 6: Vickers hardness HV10 and bending strength  $\sigma_{4pt}$  of 17ZTA materials depending on stabilizer content.

## IV. Discussion

The results presented above show that the properties of 17ZTA materials (similar in composition as currently used for biomedical implants) exhibit strong parametric sensitivity in respect of stabilizer concentration. Thus obtaining a material of both high strength and fracture resistance is only possible in a very narrow compositional range. While strength is high between 1–1.6 mol%, fracture resistance  $K_{ISB}$  shows a clear maximum in 17ZTA0.8Y, which is out of the range of maximum strength. The slight shift in the toughness maximum for  $K_{DCM}$  to higher stabilizer content may be related to the differences in R-curve behavior of the materials. The DCM value measured in non-extended cracks is probably closer to  $K_{IO}$ . As during measurement of the  $K_{ISB}$  value, cracks are extended beyond their original length during fracturing of the sample, the ISB probably better represents the rear part of the R-curve. It is still necessary to be aware of the limitations of the two testing methods. Both the ISB and DCM test start from the identical flaw geometries and residual stress fields; in ISB testing the crack is extended out of its original size by means of applied stress, thus the residual stress effect is probably less pronounced in the case of ISB. DCM is more sensitive to preparation influence, therefore grinding operations that can produce deep process zones were avoided. With regard to the moderate transformability of the materials, real “trapping” of cracks by transformation zones is not expected. It should be pointed out that both methods, DCM and ISB, were originally designed and calibrated to materials with toughness values ranging from 1–10  $\text{MPa}\sqrt{\text{m}}$  (from cemented carbide to WC-Co) with the majority of standards in the range 3–5  $\text{MPa}\sqrt{\text{m}}$ . Both methods assume median crack geometry. Towards higher toughness values and decreasing  $c/a$  ratio, a Palmqvist type crack geometry may prevail (the range of data was  $c/a: 1.94–2.85$ ). Evaluation of DCM data using the Niihara Palmqvist model<sup>26</sup> shows identical trends at an even higher toughness level (not shown). According to the test

by Quinn carried out against SEVNB<sup>25</sup>, the Niihara Model presumably leads to overestimated toughness values. Inversion of the ratio between ISB (higher at 17ZTA0.6Y and DCM higher for 17ZTA(>1.0Y) hints at contribution by different toughening mechanisms. In the microcracking regime DCM may underestimate toughness as the toughening effect becomes efficient only at larger process zones, even more so as the grain size of the material is low. Superimposed transformation and residual cooling stress together with the residual stress of the indentation as such puts the crack under compression right from the start, so that DCM may overestimate the toughness for overstabilized compositions.

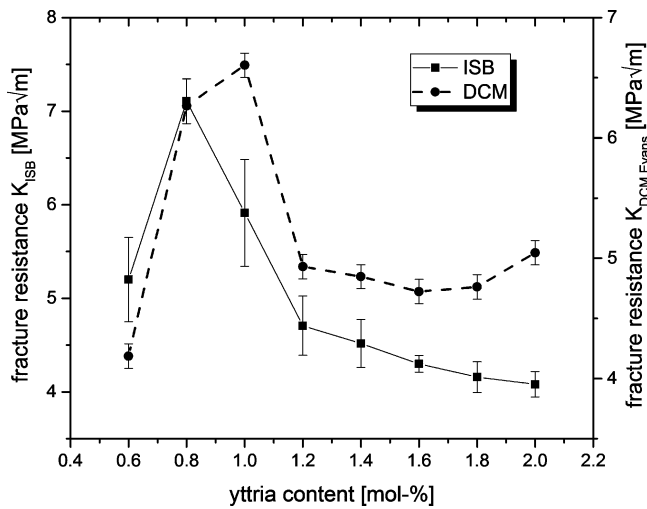


Fig. 7: Fracture resistance  $K_{ISB}$  and  $K_{DCM,Evans}$  of 17ZTA materials depending on stabilizer content.

Fig. 8 shows fracture resistance and strength depending on hydrostatic residual stress in the matrix. This plot can be interpreted as a “master curve” for ZTA development.

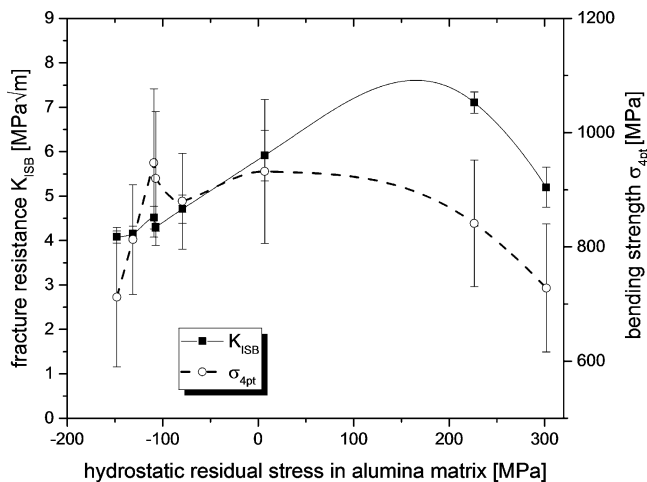


Fig. 8: Bending strength  $\sigma_{4pt}$  and fracture resistance  $K_{ISB}$  of 17ZTA materials depending on the hydrostatic residual stress in the alumina matrix..

Residual stress seems to be the dominant parameter that governs the mechanical properties of ZTA. Residual stress directly influences the formation of microcracks. Microcracks are preferentially formed if the matrix is under tension and the dispersion under compression. As shown in Fig. 2 this leads to formation of weak grain boundaries

and microcracks into the matrix material. These microcracks redistribute the crack energy over a larger volume and thus increase fracture resistance. Still a matrix under tension means a reduction of fracture resistance by crack deflection, this partially offsets the beneficial effect of microcracking<sup>25</sup>. A matrix under compression shows no microcracking at all, however, positive toughness increment based on crack deflection and little or no transformation toughening. In the range between the maxima of strength and toughness there is some synergy between the three effects. Some microcracking does occur either by existing microcracks or by microcracks that form as a consequence of stress-induced phase transformation, a moderate but significant contribution by transformation toughening is beneficial for toughness and strength and there is a moderate absolute value of crack-deflection-derived toughness – either positive on the compressive side or negative on the tensile side. The best combination of mechanical properties is achieved at in 17ZTA1.0Y with a strength of 940 MPa and a  $K_{ISB}$  of 6 MPa√m. Interestingly this is more or less the property combination found in the material of the commercially available material<sup>4</sup>. However, compared to the material prepared in this study, a considerably higher strength of 1.3 – 1.4 GPa is offered, which is an indication of an elaborate manufacturing procedure designed to minimize structural flaws. Attempts to further maximize fracture resistance and damage tolerance must result in loss of strength. Increasing the monoclinic content above the level for stress neutrality (~ 20 % monoclinic) in the matrix bears the inherent risk of low-temperature degradation derived from facilitated penetration of liquids into the bulk via the microcrack network and pronounced subcritical crack growth by the microcracks introduced by understabilization. Variation of other processing parameters such as dwell time at final temperature or change of sintering temperature which were not varied in this study will most probably also strongly affect the mechanical properties of 17ZTA materials; even more so changes in the type of starting powder used. Coarser zirconia starting powders, higher sintering temperatures and longer dwell will increase the transformability of the zirconia making a higher stabilizer content necessary to equilibrate residual stress. A reduction of the zirconia grain size either with finer starting powders or milder sintering conditions will lead to lower transformability, which can partially be compensated by lower stabilizer but may lead to a situation where the transformation is completely blocked, which would result in strong and ageing-resistant but brittle materials.

V. Conclusions

Zirconia-toughened alumina materials with a zirconia content of 17 vol% and various yttria stabilizer contents ranging from under- to overstabilized were manufactured by means of hot pressing. Materials were fully dense and their mechanical properties would fulfill the requirements of the current standard for endoprosthetic ZTA (ISO 6774 – 2). Results show the existence of two non-coinciding maxima for strength and toughness. With appropriate selection of the compositional and processing parameters, materials can be produced that are tailored for

different applications requiring high toughness for single catastrophic events or high strength and moderate fracture resistance for statically or repeatedly loaded components. More research will be required to include the influence of other compositional or processing parameters into a model, enabling knowledge-based development of ZTA materials with tailored properties.

## References

- 1 Senthil Kumar, A., Raja Durai, A., Sornakumar, T.: Machinability of hardened steel using alumina based ceramic cutting tools, *Int. J. Refract. Met. H.*, **21**, 109–117, (2003).
- 2 He, Y.J., Winnubst, A.J.A., Schipper, D.J., Bakker, P.M.V., Burggraaf, A.J., Verweij, H.: Friction and wear behaviour of ceramic-hardened steel couples under reciprocating sliding motion, *Wear*, **184**, 33–43, (1995).
- 3 Burger, W., Richter, H.G.: High strength and toughness alumina matrix composites by transformation toughening and “*in situ*” platelet reinforcement (ZPTA) – the new generation of bioceramics, *Key Eng. Mat.*, **192–195**, 545–548, (2001).
- 4 Kuntz, M.: Validation of a new high performance alumina matrix composite for use in total joint replacement, *Seminars in Arthroplasty*, **17**, 141–145, (2006).
- 5 Chevalier, J., Grandjean, S., Kuntz, M., Pezzotti, G.: Activation energy for polymorphic transformation in an advanced Alumina/Zirconia composite for arthroplastic applications, *Biomaterials*, **30**, 5279–5282, (2009).
- 6 Wang, J., Stevens, R.: Review Zirconia-toughened alumina (ZTA) ceramics, *J. Mater. Sci.*, **24**, 3421–3440, (1989).
- 7 Claussen, N.: Fracture toughness of Al<sub>2</sub>O<sub>3</sub> with an unstabilized ZrO<sub>2</sub> dispersed phase, *J. Am. Ceram. Soc.*, **59**, 49–51, (1976).
- 8 Lange, F.F.: Transformation toughening – Part 4: fabrication, fracture toughness and strength of Al<sub>2</sub>O<sub>3</sub> - ZrO<sub>2</sub> composites, *J. Mater. Sci.*, **17**, 247–254, (1982).
- 9 Hannink, R.H. J., Kelly, P.M., Muddle, B.C.: Transformation toughening in zirconia-containing ceramics, *J. Am. Ceram. Soc.*, **83**, 461–487, (2000).
- 10 Heuer, A.H., Claussen, N., Kriven, W., Rühle, W.: Stability of tetragonal ZrO<sub>2</sub> particles in ceramic matrices, *J. Am. Ceram. Soc.*, **65**, 642–650, (1982).
- 11 Gregori, G., Burger, W., Sergio, V.: Piezo-spectroscopic analysis of the residual stresses in zirconia-toughened alumina ceramics: The influence of the tetragonal-to-monoclinic transformation, *Mat. Sci. Eng. A*, **271**, 401–406, (1999).
- 12 Gutknecht, D., Chevalier, J., Garnier, V., Fantozzi, G.: Key role of processing to avoid low temperature ageing in alumina zirconia composites for orthopaedic application, *J. Eur. Ceram. Soc.*, **27**, 1547–1552, (2007).
- 13 Langlois, R., Konsztowicz, K.J.: Toughening in zirconia-toughened alumina composites with non-transforming zirconia, *J. Mater. Sci. Lett.*, **11**, 1454–1456, (1992).
- 14 Exare, C., Kiat, J.-M., Guiblin, N., Porcher, F., Petricek, V.: Structural evolution of ZTA composites during synthesis and processing, *J. Eur. Ceram. Soc.*, **35**, 1273–1283, (2015).
- 15 Sommer, F., Landfried, R., Kern, F., Gadow, R.: Mechanical properties of zirconia toughened alumina with 10–24 vol% 1.5 mol% Y-TZP reinforcement, *J. Eur. Ceram. Soc.*, **32**, 3905–3910, (2012).
- 16 Sommer, F., Landfried, R., Kern, F., Gadow, R.: Mechanical properties of zirconia toughened alumina with 10–24 vol% 1Y-TZP reinforcement, *J. Eur. Ceram. Soc.*, **32**, 4177–4184, (2012).
- 17 Kern, F., Gadow, R.: Alumina toughened zirconia from yttria coated powders, *J. Eur. Ceram. Soc.*, **32**, 3911–3918, (2012).
- 18 Evans, A.G., Charles, E.A.: Fracture toughness determinations by indentation, *J. Am. Ceram. Soc.*, **59**, 371–372, (1976).
- 19 Chantikul, P., Anstis, G.R., Lawn, B.R., Marshall, D.B.: A critical evaluation of indentation techniques for measuring fracture toughness: II, strength method, *J. Am. Ceram. Soc.*, **64**, 539–543, (1981).
- 20 Toraya, H., Yoshimura, M., Somiya, S.: Calibration curve for quantitative analysis of the monoclinic-tetragonal ZrO<sub>2</sub> system by X-ray diffraction, *J. Am. Ceram. Soc.*, **67**, C119–C121, (1984).
- 21 Kosmac, T., Wagner, R., Claussen, N.: X-ray determination of transformation depths in ceramics containing tetragonal ZrO<sub>2</sub>, *J. Am. Ceram. Soc.*, **64**, C72–C73, (1981).
- 22 McMeeking, R.M., Evans, A.G.: Mechanics of transformation-toughening in brittle materials, *J. Am. Ceram. Soc.*, **65**, 242–246, (1982).
- 23 Kelly, P.M., Rose, L.R.F.: The martensitic transformation of ceramics – its role in transformation toughening, *Progr. Mat. Sci.*, **67**, 463–557, (2002).
- 24 Quinn, G.D., Bradt, R.C.: On the vickers indentation fracture toughness test, *J. Am. Ceram. Soc.*, **90**, 673–680, (2007).
- 25 Taya, M., Hayashi, S., Kobayashi, A.S., Yoon, H.S.: Toughening of a particulate-reinforced ceramic-matrix composite by thermal residual stress, *J. Am. Ceram. Soc.*, **73**, 1382–1391, (1990).
- 26 Niihara, K.: A fracture mechanics analysis of indentation-induced palmqvist crack in ceramics, *J. Mater. Sci. Lett.*, **2**, 221–223, (1983).